



A systematical investigation of non-fullerene solar cells based on diketopyrrolopyrrole polymers as electron donor

Cheng Li, Andong Zhang, Guitao Feng, Fan Yang, Xudong Jiang, Yaping Yu, Dongdong Xia, Weiwei Li*

Beijing National Laboratory for Molecular Sciences, CAS Key Laboratory of Organic Solids, Institute of Chemistry, Chinese Academy of Sciences, Beijing, 10090, China

ARTICLE INFO

Article history:

Received 16 April 2016
Received in revised form
8 May 2016
Accepted 8 May 2016

Keywords:

Diketopyrrolopyrrole
Non-fullerene solar cells
Perylene diimide

ABSTRACT

Diketopyrrolopyrrole (DPP)-based conjugated polymers have been successfully applied in high performance field-effect transistors and fullerene-based solar cells, but show limited application in non-fullerene solar cells. In this work, we use four DPP polymers as electron donor and a perylene bisimide dye as electron acceptor to construct non-fullerene solar cells. The donors and acceptor have complementary absorption spectra in visible and near-infrared region, resulting in broad photo-response from 300 nm to 1000 nm. The solar cells were found to provide relatively low power conversion efficiencies of 1.6–2.6%, which was mainly due to low photocurrent and fill factor. Further investigation reveals that the low performance is originated from the high charge recombination in photo-active layers. Our systematical studies will help better understand the non-fullerene solar cells based on DPP polymers and inspire new researches toward efficient non-fullerene solar cells with broad photo-response.

© 2016 Elsevier B.V. All rights reserved.

1. Introduction

Perylene bisimide (PBI) derivatives with comparable electron affinities to fullerenes have been widely used as electron acceptor in non-fullerene solar cells during the last few years [1–24]. In contrast to the limited fullerene-based materials, the chemical structures of PBI compounds can be intensively engineered in terms of absorption spectra, energy levels, crystal properties and electron mobilities so as to provide the possibility to improve the photovoltaic performance. PBIs tend to form large π -stacked aggregation with size $>1 \mu\text{m}$ in thin films, but in bulk-heterojunction solar cells the domain size of 10–20 nm for the acceptor is required to provide efficient charge separation and transport [25]. In order to reduce the intermolecular interactions and avoid the strong tendency toward large crystalline aggregation of the conjugated backbone, a dimeric PBI compound, SdiPBI (Fig. 1a), was developed [19–21]. The bulk-heterojunction thin films containing SdiPBI showed favorable micro-phase separation, and hence SdiPBI and its derivatives could provide high power conversion efficiencies (PCEs)

above 8% [23].

The PCEs of solar cells depend on the physical properties of photo-active layers, such as the absorption spectra, the alignment of energy levels between donor and acceptor and the micro-phase separation. Since SdiPBI shows the narrow absorption band in the visible spectrum, the conjugated materials with absorption spectra in the near-infrared (NIR) region are required in order to sufficiently harvest sunlight. When SdiPBI as acceptor was blended with a wide band gap polymer PDBT-T1 [23] as donor, a PCE of 8.42% could be achieved but with narrow photo-response in the range of 300–700 nm, which also presented the highest performance for PBI-based solar cells. The photo-response could be further extended to 800 nm when using a well-known electron donor PBDTT-F-TT, but the cells provided a low PCE of 5.9% after applying a modified interface [19]. The low efficiency could be due to the unbalanced hole and electron mobilities (4.36×10^{-2} and $3.32 \times 10^{-5} \text{ cm}^2 \text{ V}^{-1} \text{ s}^{-1}$) of donor and acceptor, resulting in enhanced charge recombination in solar cells [19].

These studies intrigue us to search conjugated polymers with NIR absorption spectra as electron donor for SdiPBI-based non-fullerene solar cells. Our group focus on developing diketopyrrolopyrrole (DPP)-based conjugated polymers for high performance

* Corresponding author.

E-mail address: liweiwei@iccas.ac.cn (W. Li).

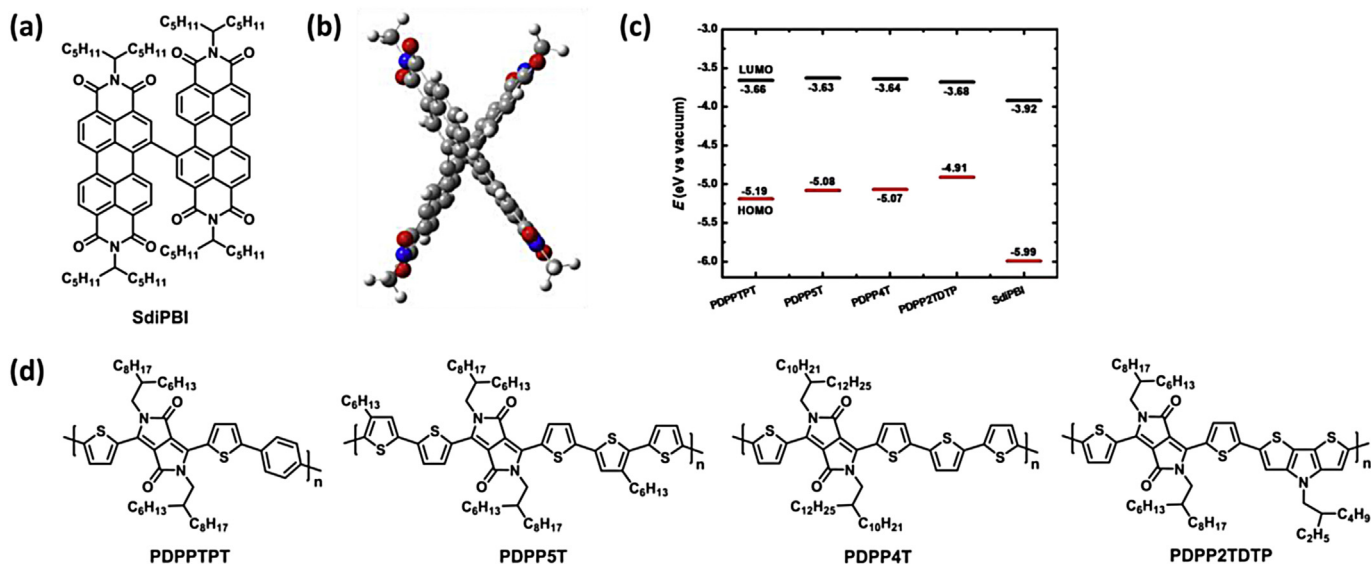


Fig. 1. (a) Chemical structures of electron acceptor SdiPBI; (b) The optimized geometry of SdiPBI obtained using DFT calculations at the B3LYP/6-31G*; (c) Energy levels of the donor and acceptor in this work; (d) Chemical structures of DPP polymers.

field-effect transistors (FETs) [26,27] and organic solar cells [28]. DPP unit has strong electron-withdrawing ability to construct small band gap conjugated polymers. By selecting electron-donating units, such as benzene [29], thiophene [30] and dithienopyrrole [31] units, the absorption onset can be easily tuned from 800 nm to 1000 nm. DPP polymers also exhibit good crystallinity and high hole mobilities above $10 \text{ cm}^2 \text{ V}^{-1} \text{ s}^{-1}$ [27,32,33]. As a result, DPP polymers as electron donor have achieved high PCEs >9% in fullerene-based solar cells [34]. Therefore, it will be interesting to study the photovoltaic properties of DPP polymer:SdiPBI systems.

In this work, we select a series of DPP polymers as donor for use in non-fullerene solar cells with SdiPBI as electron acceptor (Fig. 1). Although DPP polymers show high PCEs in fullerene-based solar cells, some studies revealed that DPP polymers performed low PCEs in non-fullerene solar cells [20,35–37]. In our previous work, we investigated the solar cells of DPP polymers as donor and a naphthalenediimide-based polymer as acceptor with PCEs below 2%, which was mainly due to the good miscibility of donor and acceptor polymers [38]. In this work, DPP polymer:SdiPBI solar cells provided better PCEs up to 2.6% with broad photo-response from 300 nm to 1000 nm. Further studies reveal that unbalanced hole and electron mobilities will enhance the charge recombination, which is mainly responsible for the low PCEs. Our results indicate that by designing new electron acceptors with high electron mobilities, DPP polymers can be used in efficient non-fullerene solar cells toward thermally stable and large-area flexible devices [39].

2. Experimental section

All chemicals were purchased from commercial suppliers and used without further purification unless otherwise specified. The four DPP polymers PDPPTPT [29], PDPP5T [40], PDPP4T [41], PDPP2TDTP [31] and the acceptor SdiPBI [9] were synthesized according to literature procedures. Poly(3-hexylthiophene) (P3HT) and [6,6]-phenyl-C₇₁-butyric acid methyl ester ([70]PCBM) were purchased from Solarmer Materials Inc.

The photovoltaic devices were fabricated with a structure of glass/ITO/ZnO/donor:acceptor/MoO₃/Ag. Zinc Acetate dehydrate

(0.5 M) and ethanolamine (0.5 M) in 2-methoxyethanol was stirred at room temperature for 2 h. The solution was spin coated at 4000 rpm for 60 s onto precleaned, patterned ITO substrates and the thin film was thermal annealed at 150 °C for 10 min to form ZnO layer [42]. The photoactive layer was deposited by spin coating the DPP polymer:SdiPBI in chloroform solution with appropriate amount of processing additive such as 1,8-diiodooctane (DIO) or *ortho*-dichlorobenzene (*o*-DCB) in air. The photoactive layers based on P3HT:[70]PCBM (1:1) were fabricated from *o*-DCB solution (30 mg mL^{-1}) at 1000 rpm in air and thermal annealed at 150 °C for 10 min in N₂ filled glove box. MoO₃ (10 nm) and Ag (100 nm) were deposited by vacuum evaporation at ca. 4×10^{-5} Pa as the back electrode. The active area of the cells was 0.04 cm². The *J*-*V* characteristics were measured by a Keithley 2400 source meter unit under AM1.5G spectrum from a solar simulator (enlitech model SS-F5-3A). Solar simulator illumination intensity was determined at 100 mW/cm² using a monocrystal silicon reference cell with KG5 filter.

Short circuit currents under AM1.5G conditions were estimated from the spectral response and convolution with the solar spectrum. The external quantum efficiency was measured by a Solar Cell Spectral Response Measurement System QE-R3011 (Enli Technology Co., Ltd.). The thickness of the active layers in the photovoltaic devices was measured on a Veeco Dektak XT profilometer.

Density functional theory (DFT) calculations were performed at the B3LYP/6-31G* level of theory by using the Gaussian 09 program package. AFM images were recorded using a digital instruments nanoscope IIIA multimode atomic force microscope in tapping mode.

The carrier mobilities were measured by space charge limit current (SCLC), where the device configuration of ITO/PEDOT:PSS/active layer/Au was used for hole-only devices and ITO/ZnO/active layer/LiF/Al was used for electron-only devices. The mobilities were calculated from the slope of the $J^{1/2}$ -*V* curves, by fitting the dark current according to the model of a single carrier SCLC equation: $J = 9\epsilon_0\epsilon_r\mu_h(\mu_e)V^2/8d^3$, where *J* is the measured current density, ϵ_0 is the permittivity of free space, ϵ_r is the relative dielectric constant of the transport material, μ is the mobility, *d* is the thickness of the active layer. *V* is the difference between the applied voltage and the offset voltage.

3. Results and discussion

3.1. Chemical structures, optical and electrochemical properties

The chemical structures of the DPP polymers and SdiPBI are shown in Fig. 1. From DFT calculations, the molecular SdiPBI has highly twisted 3D geometries (Fig. 1b), which could suppress the self-aggregation of PBI units and meanwhile improve the isotropic electron transport. Four DPP polymers were selected as electron donor, in which the DPP core was flanked with different electron-donating units, from benzene (PDPPTPT) to terthiophene (PDPP5T), bithiophene (PDPP4T) and dithienopyrrole (PDPP2TDTP) (Fig. 1d). Thieryl units were used as bridges to connect the DPP core and donor groups. All these polymers have been reported in fullerene-based solar cells with high photocurrent and PCEs up to 7% [29,31,40,41].

The optical absorption spectra of the donor polymers and SdiPBI are shown in Fig. 2 and the optical band gap (E_g) is summarized at Table 1. SdiPBI presents the absorption spectra from 400 nm to 600 nm, while the DPP polymers have the complementary absorption spectra in NIR region. PDPPTPT with phenyl units as weak donor shows absorption onset at 810 nm with E_g of 1.53 eV. When enhancing the electron-donating ability, the band gaps of PDPP5T, PDPP4T and PDPP2TDTP reduce to 1.45 eV, 1.43 eV and 1.27 eV respectively. The absorption spectra of the blended thin films of DPP polymer:SdiPBI with the ratio of 1:1 is also present in Fig. 2b, in which the absorption contribution from the donor and SdiPBI can be clearly distinguished. It is also notable that the absorption intensity of SdiPBI is much lower than that of DPP polymers, indicating the relatively low absorption coefficient of SdiPBI.

The energy levels of the DPP polymers and SdiPBI that were determined from cyclic voltammetry (CV) measurement are shown in Fig. 1c and summarized at Table 1. The DPP polymers show the similar lowest unoccupied molecular orbital (LUMO) levels of -3.63 to -3.68 eV, while SdiPBI has LUMO level of -3.92 eV. Therefore, the LUMO offset between the polymer and SdiPBI is 0.24 – 0.29 eV, which is close to 0.3 eV [43]. In addition, the DPP polymers provide the highest occupied molecular orbital (HOMO) levels of -4.91 to -5.19 eV, which is much lower than that of SdiPBI (-5.99 eV). The HOMO and LUMO offsets between the DPP polymers and SdiPBI can provide enough driving force for exciton dissociation into free charges.

3.2. Photovoltaic properties

Bulk-heterojunction solar cells were fabricated by using DPP

Table 1
Optical and energy levels of the DPP polymers and SdiPBI.

Polymer	E_g^{film} (eV)	E_{LUMO} (eV)	E_{HOMO} (eV) ^a	ΔE_{LUMO} (eV) ^b
PDPPTPT ^c	1.53	-3.66	-5.19	0.26
PDPP5T ^d	1.45	-3.63	-5.08	0.29
PDPP4T ^e	1.43	-3.64	-5.07	0.28
PDPP2TDTP ^f	1.23	-3.68	-4.91	0.24
SdiPBI ^g	2.07	-3.92	-5.99	–

^a $E_{\text{HOMO}} = E_{\text{LUMO}}(\text{polymer}) - E_g^{\text{film}}$.

^b $\Delta E_{\text{LUMO}} = E_{\text{LUMO}}(\text{polymer}) - E_{\text{LUMO}}(\text{SdiPBI})$.

^c Ref. [30].

^d Ref. [35].

^e Ref. [41].

^f Ref. [31].

^g Ref. [9].

polymers as electron donor and SdiPBI as electron acceptor with an inverted device structure of ITO/ZnO/DPP polymer:SdiPBI/MoO₃/Ag. The photoactive layers were carefully optimized according to the processing parameters including solvent, the amount of additive (Tables S1–S5, Fig. S1) and the ratio of donor to acceptor (Tables S5–S8, Fig. S2). All the cells show the best performance when the ratio of donor to acceptor is 1:1. The optimized performance of the solar cells is shown in Fig. 3 and the photovoltaic parameters are summarized at Table 2.

PDPPTPT:SdiPBI cells show the best PCE of 2.1% with short circuit current density (J_{sc}) of 5.5 mA cm^{-2} , open circuit voltage (V_{oc}) of 0.88 V and fill factor (FF) of 0.43. When SdiPBI is blended with PDPP5T and PDPP4T, the J_{sc} s are enhanced to 8.9 mA cm^{-2} and 7.5 mA cm^{-2} , but V_{oc} s are reduced to 0.63 V and 0.74 V, resulting in similar PCEs of 2.3% and 2.6% as PDPPTPT:SdiPBI cell. PDPP2TDTP:SdiPBI cell shows similar J_{sc} and FF but with very low V_{oc} of 0.50, and thus provides the lowest PCE of 1.6%. The J_{sc} s of these cells are also reflected by their external quantum efficiencies (EQE) as shown in Fig. 3b. All the cells exhibit two distinct spectra that correlate to the contribution from SdiPBI and DPP polymers. PDPPTPT:SdiPBI cell shows the photo-response from 300 nm to 800 nm with the EQE below 0.25, while PDPP2TDTP:SdiPBI cell has the broad spectra from 300 nm to 1000 nm with the maximum EQE of 0.30. PDPP5T-based cells provide the best EQE up to 0.35, corresponding to the highest J_{sc} of 8.9 mA cm^{-2} in these cells. Although the cells show the broad photo-response, the EQEs are still much lower than those of fullerene-based cells, which can explain their relatively low J_{sc} s and PCEs. In addition, the FF of these non-fullerene solar cells is also below 0.50, which is much lower than those of DPP polymer solar cells with typical FF above 0.65 when using fullerene derivatives as electron acceptor [41]. We also

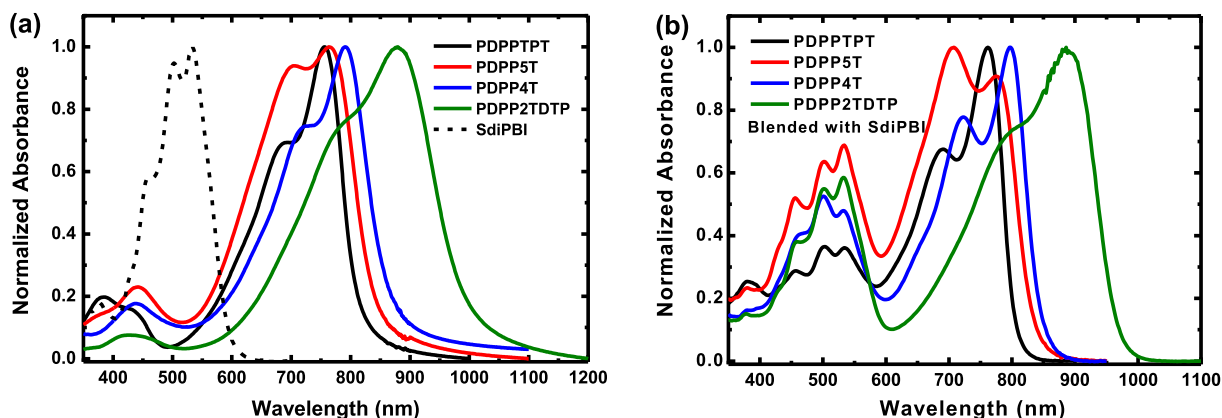


Fig. 2. (a) Absorption spectra of the pure DPP polymers and SdiPBI in solid state films and (b) of the blended thin films of DPP polymer:SdiPBI (1:1) spin coated from CHCl₃ solution.

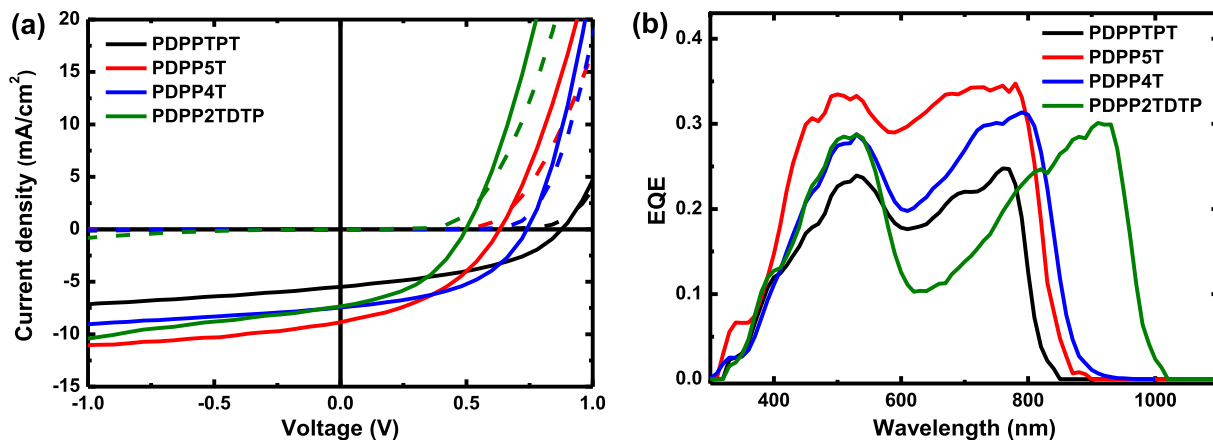


Fig. 3. (a) J - V characteristics in dark (dashed lines) and under white light illumination (solid lines) of optimized solar cells of DPP polymers blended with SdiPBI (1:1) fabricated from CHCl_3 with 2.5% DIO as additive for PDPP5T and PDPP2TDTP, and CHCl_3 with 10% *o*-DCB as additive for PDPPTPT and PDPP4T. (b) EQE of the same devices.

Table 2

Solar cell parameters of optimized inverted solar cells of DPP polymer:SdiPBI.

Polymer ^a	J_{sc} ^b [mA cm ⁻²]	V_{oc} [V]	FF	PCE [%]	E_{loss} ^c (eV)
PDPPTPT	5.5	0.88	0.43	2.1	0.65
PDPP5T	8.9	0.63	0.41	2.3	0.82
PDPP4T	7.5	0.74	0.47	2.6	0.69
PDPP2TDTP	7.4	0.50	0.43	1.6	0.73
P3HT ^d	8.1	0.57	0.60	2.7	1.28

^a Ratio of donor to acceptor is 1:1. Optimized spin coating solvent for active layer is CHCl_3 with 2.5% DIO as additive for PDPP5T and PDPP2TDTP, and CHCl_3 with 10% *o*-DCB as additive for PDPPTPT and PDPP4T.

^b J_{sc} as calculated by integrating the EQE spectrum with the AM1.5 G spectrum.

^c $E_{loss} = E_g - qV_{oc}$.

^d With [70]PCBM. The thickness of the active layer is 100 nm.

fabricated the P3HT:[70]PCBM cells as shown in Fig. S3 and the results were summarized in Table 2. The cells have similar PCEs of 2.7% but with narrow photon-response only up to 700 nm (Fig. S3b). However, P3HT:PCBM cells show EQE above 0.5 in the visible light region, which is much higher than those of non-fullerene solar cells.

3.3. Investigation of charge transports

It is worth to further study the charge separation and transport in these non-fullerene solar cells in order to understand their low device performance. Firstly, the energy loss (E_{loss}) [44], that is defined as the difference between E_g and qV_{oc} , was evaluated in these cells, as shown in Table 2. All the cells have the E_{loss} above 0.6 eV with the highest value of 0.82 eV, which can be recognized to provide sufficient driving force for charge separation. In addition, P3HT:PCBM cells provide a large E_{loss} of 1.28 eV that will greatly limit the performance of solar cells.

The charge transport properties of the cells were investigated by space charge limited current (SCLC) measurement, as shown in Fig. S3 and Table 3. The results of the DPP polymer:[70]PCBM cells were also present for comparison. All the DPP polymers show similar hole mobilities of 10^{-4} cm² V⁻¹ s⁻¹, in which DPP polymer:[70]PCBM has slightly higher mobilities than those of non-fullerene solar cells. In addition, SdiPBI presents electron mobilities around 10^{-5} cm² V⁻¹ s⁻¹ in blended thin films, while the electron mobilities of [70]PCBM in blended thin films were $\sim 10^{-4}$ cm² V⁻¹ s⁻¹. As consequence, DPP polymer:SdiPBI cells present unbalanced hole and electron mobilities compared to [70]PCBM-based cells (Table 1), which will enhance the charge

Table 3

Hole and electron mobility by SCLC measurement.

Active layer	μ_h (cm ² V ⁻¹ s ⁻¹)	μ_e (cm ² V ⁻¹ s ⁻¹)	μ_h/μ_e
PDPPTPT:SdiPBI	2.92×10^{-4}	1.35×10^{-5}	21.6
PDPP5T:SdiPBI	3.77×10^{-4}	1.41×10^{-5}	26.7
PDPP4T:SdiPBI	5.47×10^{-4}	1.38×10^{-5}	39.6
PDPP2TDTP:SdiPBI	3.67×10^{-4}	6.60×10^{-6}	55.6
PDPPTPT:[70]PCBM ^a	6.21×10^{-4}	1.66×10^{-4}	3.74
PDPP5T:[70]PCBM ^a	7.13×10^{-4}	8.64×10^{-5}	8.25
PDPP4T:[70]PCBM ^a	8.12×10^{-4}	1.83×10^{-4}	4.44
PDPP2TDTP:[70]PCBM ^a	8.14×10^{-4}	2.25×10^{-4}	3.62

^a The ratio of donor to [70]PCBM is 1:2 and the thin films were fabricated by using optimized condition according to the literatures [30,31,35,41].

recombination of these cells. These could explain the low J_{sc} s and FF. These results also reveal that improving the electron mobility of acceptors is the possible route to improve the DPP-based non-fullerene solar cells.

In order to further study the charge recombination in these non-fullerene cells, the charge dissociation probability $P(E, T)$ was investigated according to the reported method. As shown in Fig. 4a, the photocurrent density J_{ph} (defined by $J_L - J_D$, J_L and J_D are light and dark current densities) is plotted against effective voltage V_{eff} (defined by $V_0 - V$, V_0 is the voltage where $J_{ph} = 0$) on a logarithmic scale [45]. V_{eff} reflects the applied voltage used for charge exaction, in which high V_{eff} can provide enough driving force for charge dissociation and therefore has minimal recombination. In these SdiPBI-based cells, J_{ph} cannot reach the saturation values, indicating the strong charge recombination. By using the J_{ph} at 2 V and the J_{ph} at the maximum power output point, the $P(E, T)$ can be calculated as 49.4%, 47.8%, 57.8% and 49.0% for PDPPTPT, PDPP5T, PDPP4T and PDPP2TDTP-based cells respectively. It should be note that, since the J_{ph} at 2 V is the unsaturated values, the real $P(E, T)$ should be even lower than the calculated values as shown in Fig. 4a. The $P(E, T)$ is rather low compared to those efficient fullerene-based solar cells, indicating poor exciton dissociation and charge collection [45].

The short circuit current under different light intensities was also measured to study charge recombination, as shown in Fig. 4b. The relationship between J_{sc} and light intensity (P) can be described by the formula of $J_{sc} \propto P^S$ [46]. $S = 1$ indicates that all free charges are transported and collected at the electrodes, while $S < 1$ indicates charge recombination. In these SdiPBI-based cells, S is in the range of 0.83–0.97, especially for PDPP5T and PDPP2TDTP with S of 0.90 and 0.83. These results reveal that DPP polymer:SdiPBI thin films have strong charge recombination, which is consistent with

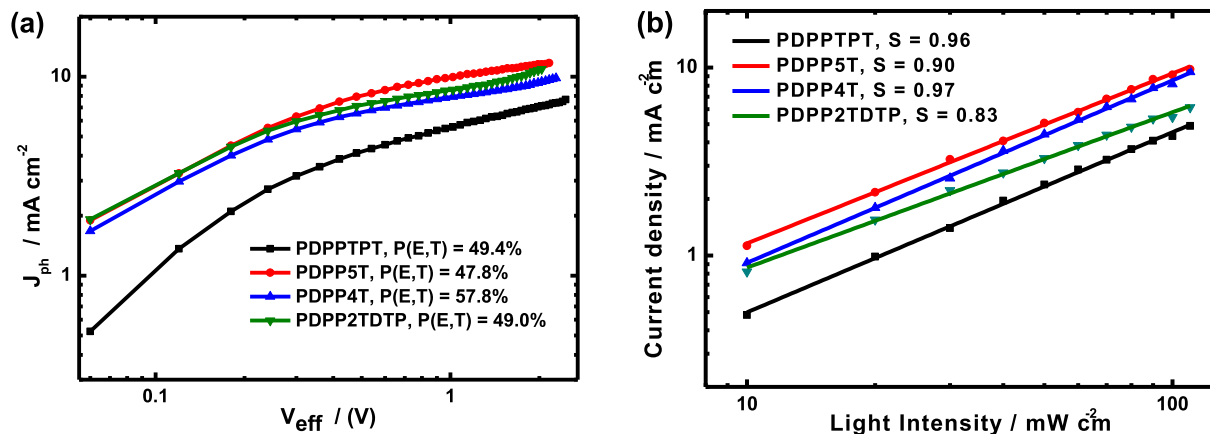


Fig. 4. (a) Photocurrent density J_{ph} versus effective voltage V_{eff} . (b) Light intensity dependence of J_{sc} .

the SCLC and J_{ph} measurement.

We further studied the morphology of blended thin films by atomic force microscopy (AFM), as shown in Fig. 5. All thin films show smooth surface with roughness from 0.89 nm to 2.15 nm. This may indicate the well-mixed phase between donor and acceptor, which can enhance the possibility of charge recombination. The observation is similar to the DPP polymer donor:polymer acceptor in our previous work [38].

4. Conclusions

In conclusion, non-fullerene solar cells based on DPP

polymers as electron donor and a PBI-based compound as electron acceptor were studied in this work. The DPP polymers have the complementary absorption spectra with the electron acceptor, resulting in broad photo-response from 300 nm to 1000 nm in solar cells. The solar cells exhibit low PCEs of 1.6–2.6%, which is mainly due to the high charge recombination. The systematical investigation in this work will be helpful to understand the physical process in these DPP polymer solar cells. With the consideration of broad absorption spectra, high charge carrier mobilities and good crystallinity, we believe that DPP polymers as donor will show promising application in non-fullerene solar cells.

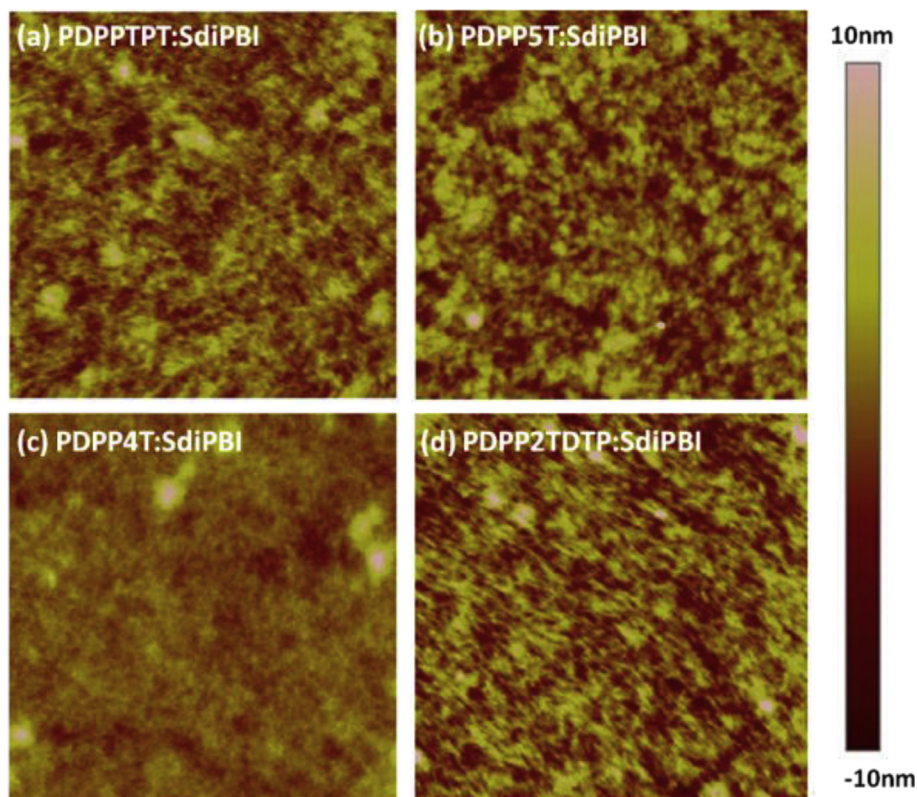


Fig. 5. AFM height image ($3 \times 3 \mu\text{m}^2$) of optimized DPP polymer:SdiPBI (1:1) active layers spin coated from CHCl_3 with 2.5% DIO as additive for PDPP5T and PDPP2TDTP, and CHCl_3 with 10% *o*-DCB as additive for PDPPTPT and PDPP4T. (a) PDPPTPT, (b) PDPP5T, (c) PDPP4T and (d) PDPP2TDTP. The root mean square (RMS) roughness values are 1.89 nm, 2.02 nm, 0.89 nm and 2.15 nm respectively.

Acknowledgment

This work was supported by the Recruitment Program of Global Youth Experts of China. The work was further supported by the National Natural Science Foundation of China (21574138) and the Strategic Priority Research Program (XDB12030200) of the Chinese Academy of Sciences.

Appendix A. Supplementary data

Supplementary data related to this article can be found at <http://dx.doi.org/10.1016/j.orgel.2016.05.011>.

References

- [1] C. Zhan, J. Yao, *Chem. Mater.* 28 (2016) 1948–1964.
- [2] X. Zhan, Z. Tan, B. Domercq, Z. An, X. Zhang, S. Barlow, Y. Li, D. Zhu, B. Kippelen, S.R. Marder, *J. Am. Chem. Soc.* 129 (2007) 7246–7247.
- [3] E. Zhou, J. Cong, Q. Wei, K. Tajima, C. Yang, K. Hashimoto, *Angew. Chem. Int. Ed.* 50 (2011) 2799–2803.
- [4] Y. Zhou, T. Kurosawa, W. Ma, Y. Guo, L. Fang, K. Vandewal, Y. Diao, C. Wang, Q. Yan, J. Reinspach, J. Mei, A.L. Appleton, G.I. Koleilat, Y. Gao, S.C.B. Mannsfeld, A. Salleo, H. Ade, D. Zhao, Z. Bao, *Adv. Mater.* 26 (2014) 3767–3772.
- [5] S. Li, H. Zhang, W. Zhao, L. Ye, H. Yao, B. Yang, S. Zhang, J. Hou, *Adv. Energy Mater.* 6 (2016) 1501991.
- [6] Y. Zhang, Q. Wan, X. Guo, W. Li, B. Guo, M. Zhang, Y. Li, *J. Mater. Chem. A* 3 (2015) 18442–18449.
- [7] S. Nam, S.G. Hahm, H. Han, J. Seo, C. Kim, H. Kim, S.R. Marder, M. Ree, Y. Kim, *ACS Sustain. Chem. Eng.* 4 (2016) 767–774.
- [8] B. Jiang, X. Zhang, C. Zhan, Z. Lu, J. Huang, X. Ding, S. He, J. Yao, *Polym. Chem.* 4 (2013) 4631–4638.
- [9] W. Jiang, L. Ye, X. Li, C. Xiao, F. Tan, W. Zhao, J. Hou, Z. Wang, *Chem. Commun.* 50 (2014) 1024–1026.
- [10] R. Shivanna, S. Shoaee, S. Dimitrov, S.K. Kandappa, S. Rajaram, J.R. Durrant, K.S. Narayan, *Energy Environ. Sci.* 7 (2014) 435–441.
- [11] J. Yi, Y. Wang, Q. Luo, Y. Lin, H. Tan, H. Wang, C.-Q. Ma, *Chem. Commun.* 52 (2016) 1649–1652.
- [12] Y. Zhong, M.T. Trinh, R. Chen, G.E. Purdum, P.P. Khlyabich, M. Sezen, S. Oh, H. Zhu, B. Fowler, B. Zhang, W. Wang, C.-Y. Nam, M.Y. Sfeir, C.T. Black, M.L. Steigerwald, Y.-L. Loo, F. Ng, X.Y. Zhu, C. Nuckolls, *Nat. Commun.* 6 (2015) 8242.
- [13] X. Zhang, Z. Lu, L. Ye, C. Zhan, J. Hou, S. Zhang, B. Jiang, Y. Zhao, J. Huang, S. Zhang, Y. Liu, Q. Shi, Y. Liu, J. Yao, *Adv. Mater.* 25 (2013) 5791–5797.
- [14] Z. Lu, B. Jiang, X. Zhang, A. Tang, L. Chen, C. Zhan, J. Yao, *Chem. Mater.* 26 (2014) 2907–2914.
- [15] R. Singh, E. Aluicio-Sarduy, Z. Kan, T. Ye, R.C.I. MacKenzie, P.E. Keivanidis, *J. Mater. Chem. A* 2 (2014) 14348–14353.
- [16] P.E. Hartnett, A. Timalina, H.S.S.R. Matte, N. Zhou, X. Guo, W. Zhao, A. Facchetti, R.P.H. Chang, M.C. Hersam, M.R. Wasielewski, T.J. Marks, *J. Am. Chem. Soc.* 136 (2014) 16345–16356.
- [17] P. Cheng, X. Zhao, W. Zhou, J. Hou, Y. Li, X. Zhan, *Org. Electron.* 15 (2014) 2270–2276.
- [18] N. Liang, K. Sun, Z. Zheng, H. Yao, G. Gao, X. Meng, Z. Wang, W. Ma, J. Hou, *Adv. Energy Mater.* (2016), <http://dx.doi.org/10.1002/aenm.201600060>.
- [19] Y. Zang, C.-Z. Li, C.-C. Chueh, S.T. Williams, W. Jiang, Z.-H. Wang, J.-S. Yu, A.K.Y. Jen, *Adv. Mater.* 26 (2014) 5708–5714.
- [20] L. Ye, W. Jiang, W. Zhao, S. Zhang, Y. Cui, Z. Wang, J. Hou, *Org. Electron.* 17 (2015) 295–303.
- [21] Y. Fu, Q. Yang, Y. Deng, W. Jiang, Z. Wang, Y. Geng, Z. Xie, *Org. Electron.* 18 (2015) 24–31.
- [22] D. Sun, D. Meng, Y. Cai, B. Fan, Y. Li, W. Jiang, L. Huo, Y. Sun, Z. Wang, *J. Am. Chem. Soc.* 137 (2015) 11156–11162.
- [23] D. Meng, D. Sun, C. Zhong, T. Liu, B. Fan, L. Huo, Y. Li, W. Jiang, H. Choi, T. Kim, J.Y. Kim, Y. Sun, Z. Wang, A.J. Heeger, *J. Am. Chem. Soc.* 138 (2016) 375–380.
- [24] G. Feng, Y. Xu, J. Zhang, Z. Wang, Y. Zhou, Y. Li, Z. Wei, C. Li, W. Li, *J. Mater. Chem. A* (2016), <http://dx.doi.org/10.1039/C5TA10430K>.
- [25] J.J. Dittmer, E.A. Marsaglia, R.H. Friend, *Adv. Mater.* 12 (2000) 1270–1274.
- [26] C. Xiao, G. Zhao, A. Zhang, W. Jiang, R.A.J. Janssen, W. Li, W. Hu, Z. Wang, *Adv. Mater.* 27 (2015) 4963–4968.
- [27] Y. Ji, C. Xiao, Q. Wang, J. Zhang, C. Li, Y. Wu, Z. Wei, X. Zhan, W. Hu, Z. Wang, R.A.J. Janssen, W. Li, *Adv. Mater.* 28 (2016) 943–950.
- [28] W. Li, K.H. Hendriks, M.M. Wienk, R.A.J. Janssen, *Acc. Chem. Res.* 49 (2016) 78–85.
- [29] W. Li, K.H. Hendriks, A. Furlan, W.S.C. Roelofs, S.C.J. Meskers, M.M. Wienk, R.A.J. Janssen, *Adv. Mater.* 26 (2014) 1565–1570.
- [30] K.H. Hendriks, G.H.L. Heintges, V.S. Gevaerts, M.M. Wienk, R.A.J. Janssen, *Angew. Chem. Int. Ed.* 52 (2013) 8341–8344.
- [31] K.H. Hendriks, W. Li, M.M. Wienk, R.A.J. Janssen, *J. Am. Chem. Soc.* 136 (2014) 12130–12136.
- [32] Z. Yi, S. Wang, Y. Liu, *Adv. Mater.* 27 (2015) 3589–3606.
- [33] J.Y. Back, H. Yu, I. Song, I. Kang, H. Ahn, T.J. Shin, S.-K. Kwon, J.H. Oh, Y.-H. Kim, *Chem. Mater.* 27 (2015) 1732–1739.
- [34] H. Choi, S.-J. Ko, T. Kim, P.-O. Morin, B. Walker, B.H. Lee, M. Leclerc, J.Y. Kim, A.J. Heeger, *Adv. Mater.* 27 (2015) 3318–3324.
- [35] W. Li, W.S.C. Roelofs, M. Turbiez, M.M. Wienk, R.A.J. Janssen, *Adv. Mater.* 26 (2014) 3304–3309.
- [36] J.W. Jung, W.H. Jo, *Polym. Chem.* 6 (2015) 4013–4019.
- [37] A. Zhang, Q. Wang, R.A.A. Bovee, C. Li, J. Zhang, Y. Zhou, Z. Wei, Y. Li, R.A.J. Janssen, Z. Wang, W. Li, *J. Mater. Chem. A* (2016), <http://dx.doi.org/10.1039/C6TA00962J>.
- [38] C. Li, A. Zhang, Z. Wang, F. Liu, Y. Zhou, T.P. Russell, Y. Li, W. Li, *RSC Adv.* 6 (2016) 35677–35683.
- [39] W. Zhao, D. Qian, S. Zhang, S. Li, O. Inganäs, F. Gao, J. Hou, Fullerene-free polymer solar cells with over 11% efficiency and excellent thermal stability, *Adv. Mater.* (2016), <http://dx.doi.org/10.1002/adma.201600281>.
- [40] W. Li, W.S.C. Roelofs, M.M. Wienk, R.A.J. Janssen, *J. Am. Chem. Soc.* 134 (2012) 13787–13795.
- [41] W. Li, K.H. Hendriks, A. Furlan, W.S.C. Roelofs, M.M. Wienk, R.A.J. Janssen, *J. Am. Chem. Soc.* 135 (2013) 18942–18948.
- [42] Y. Sun, J.H. Seo, C.J. Takacs, J. Seifert, A.J. Heeger, *Adv. Mater.* 23 (2011) 1679–1683.
- [43] C.J. Brabec, C. Winder, N.S. Sariciftci, J.C. Hummelen, A. Dhanabalan, P.A. van Hal, R.A.J. Janssen, *Adv. Funct. Mater.* 12 (2002) 709–712.
- [44] W. Li, K.H. Hendriks, A. Furlan, M.M. Wienk, R.A.J. Janssen, *J. Am. Chem. Soc.* 137 (2015) 2231–2234.
- [45] L. Lu, T. Xu, W. Chen, E.S. Landry, L. Yu, *Nat. Photon.* 8 (2014) 716–722.
- [46] P. Schilinsky, C. Waldauf, C.J. Brabec, *Appl. Phys. Lett.* 81 (2002) 3885–3887.